Revista Brasileira de Farmacognosia (2022) 32:111–121
https://doi.org/10.1007/s43450-022-00230-4

ORIGINAL ARTICLE

Curine Ameliorates Lipopolysaccharide-Induced Acute Lung Injury by Downregulating the TLR4/MD-2/NF-κB(p65) Signaling Pathway

Larissa A. M. Paiva Ferreira[1] · Laércia K. D. Paiva Ferreira[1] · Talissa M. Monteiro[1] · Francisco A. A. F. Gadelha[1] · Louise M. de Lima[1] · Mayara dos Santos Maia[2] · Marcus Tullius Scotti[2] · Jaime Ribeiro-Filho[3] · Celidarque da S. Dias[4] · Marcia Regina Piuvezam[1]

Received: 7 September 2021 / Accepted: 3 January 2022 / Published online: 28 January 2022

Abstract

Acute lung injury is characterized by alveolar-capillary barrier rupture, neutrophil-mediated airway inflammation, and tissue hypoxia. Since no effective pharmacotherapy is currently available, alternatives to improve its condition are mandatory. Recent studies demonstrated that curine, a bisbenzylisoquinoline alkaloid from *Chondrodendron platyphyllum* (A.St.-Hil.) Miers, Menispermaceae, with anti-allergic and anti-inflammatory properties, inhibited lipopolysaccharide-mediated acute pulmonary response in mice. Therefore, this study aimed to investigate curine's mechanism of action in a lipopolysaccharide-induced acute lung injury model. Curine inhibited the recruitment of inflammatory cells to the bronchoalveolar lavage fluid, mainly dependent on neutrophil migration, and restored the pulmonary architecture by reducing edema, vascular permeability, and the total protein content as well as the wet/dry ratio of the lung. Curine also decreased the TNF-α, IL-1β, and IL-6 production through downregulating the toll-like receptor 4 receptor expression and the nuclear factor-kappa B (p65) phosphorylation. *In silico* analysis demonstrated that curine made hydrophobic interactions with the Leu78, Ile80, Phe121, Ile124, Phe126, and Ile 152 amino acids of the hydrophobic cavity of the MD-2 receptor. This curine interaction presented stability during the simulation, remaining linked to the active site, indicating an antagonistic interaction with the molecular complex lipopolysaccharides/toll-likereceptor/4 myeloid differentiation factor 2.

Keywords Neutrophils · Cytokines · Lung injury experimental model · TLR4 · Transcriptional factor-κB

Introduction

Acute lung injury (ALI) and its most severe form, acute respiratory discomfort syndrome (ARDS), are characterized by neutrophil-mediated acute lung inflammation, loss of alveolar-capillary membrane integrity, and reduction of lung compliance (Cheung et al. 2017). These events alter the ventilation/perfusion combination, gas exchange, and the mechanical properties of the lung compromising the lung compliance, airway resistance, and the pressure-volume curve (Cheung et al. 2017). The ARDS develops either by direct (pulmonary) or indirect (extrapulmonary) causes according to the site of infection (Fan et al. 2018). While direct lung injury occurs due to infection of the respiratory tract by microorganisms such as viruses, fungi, and bacteria, indirect lung injury occurs when these agents reach the lung through the bloodstream, as observed in sepsis (Rezoagli et al. 2017). Lipopolysaccharide (LPS), a Gram-negative bacteria membrane constituent, has been extensively used in murine models of ALI because it induces the entire pathological picture characteristic of this disease (Proudfoot et al. 2011). Global data indicate that ARDS is responsible for 10% of intensive care unit admissions, representing more than three million ARDS patients annually, with a 40% rate of mortality (Bellani et al.

Larissa A. M. Paiva Ferreira and Laércia K. D. Paiva Ferreira contributed equally to this work.

✉ Marcia Regina Piuvezam
mrpiuvezam@ltf.ufpb.br

[1] Laboratório de Imunofarmacologia, Programa de Pós-graduação em Produtos Naturais e Sintéticos, Universidade Federal da Paraíba, João Pessoa, PB, Brazil

[2] Laboratório de Quimioinformática, Programa de Pós-graduação em Produtos Naturais e Sintéticos, Universidade Federal da Paraíba, João Pessoa, PB, Brazil

[3] Instituto Gonçalo Moniz, Fundação Oswaldo Cruz, IGM-FIOCRUZ/BA, Salvador, BA, Brazil

[4] Departamento de Ciências Farmacêuticas, Universidade Federal da Paraíba, João Pessoa, PB, Brazil

2016; Rezoagli et al. 2017). The activated neutrophil in the airway lumen is a hallmark of disease progression. Studies have shown that the activation of this cell population in ARDS occurs when a microorganism binds to the toll-like receptor complex (TLR-4/CD14/MD-2). These interactions lead to signaling pathways associated with the nuclear factor-kappa B (NF-κB) activation and pro-inflammatory gene transcription (Yang et al. 2018). Thus, activated neutrophils release several mediators that induce alveolar epithelial injury, including cytokines, lipid mediators, reactive oxygen species (ROS), proteases, elastases, matrix metalloproteinases, myeloperoxidase (MPO), and cationic peptides such as defensins (Albiger et al. 2007; Yang et al. 2018). Besides, evidence has demonstrated that the formation of neutrophil extracellular traps (NETs) contributes to tissue injury via the induction of necrosis, apoptosis, and autophagy (Yang et al. 2018).

The current basis for the treatment of ARDS is mechanical ventilation without a standard pharmacotherapy. Thus, new effective therapeutic strategies capable of modulating the inflammation-associated tissue damage in ARDS are a demanding need. In this context, medicinal plants used to treat inflammatory diseases in traditional medicine represent important sources of bioactive compounds with pharmacological potential (Petrovska 2012).

Chondrodendron platyphyllum (A.St.-Hil.) Miers, Menispermaceae, a medicinal plant found in Northeastern Brazil, popularly known as "abútua," is used for the relief of fever, anemia, and diarrhea (Dias et al. 2002). Chemical analyses using the root showed that this plant is rich in bisbenzylisoquinoline alkaloids (BBA), such as curine (**1**), isocurine, and 12-*O*-methylcurine (Dias et al. 2002; Guedes et al. 2002). Our research group has been studying curine (**1**), and its anti-allergic, analgesic, and anti-inflammatory effects have been demonstrated (Dias et al. 2002; Guedes et al. 2002; Medeiros et al. 2011; Leite et al. 2014; Ribeiro-Filho et al. 2013, 2019). Its mechanism of action involves inhibition of calcium channels (Dias et al. 2002; Guedes et al. 2002; Medeiros et al. 2011). Previous studies have shown that curine (**1**) has low toxicity without altering biochemical, hematological, physical, and behavioral parameters as well as no gastric tissue damage (Ribeiro-Filho et al. 2013). Curine also promoted vasodilatation, reduced intracellular Ca2+ in smooth muscle cells, blocked type 1.2 calcium channels, inhibited the production of CysLT and PGD2 by mast cells, and extended the animal's survival time in the anaphylactic shock reaction (Medeiros et al. 2011; Ribeiro-Filho et al. 2014). Ribeiro-Filho et al. (2013) described the anti-allergic effects of curine using an experimental model of ovalbumin-induced allergic asthma. In this study, the authors demonstrated that the alkaloid inhibited eosinophil migration, lipid body formation, decreased eotaxin, and IL-13 production into the bronchoalveolar lavage. Also, the same research group demonstrated the anti-edematogenic effect of curine in an experimental model of paw edema induced by phlogistic agents by decreasing vascular permeability. Besides, curine presented analgesic activity by inhibiting the PGE2 production without interfering with the expression of COX-2(Leite et al. 2014).

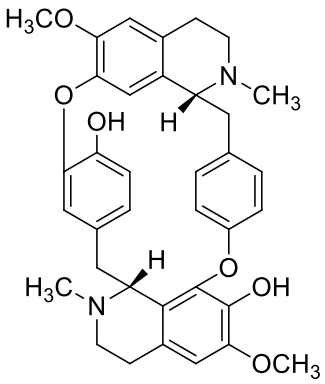

1

The treatment with curine (**1**) in an experimental model of allergic asthma was found to inhibit eosinophilic inflammation, airway hyperresponsiveness (AHR), lipid body formation, and the production of type 2 cytokines. Also, the similarity between the anti-allergic effect of curine and verapamil (a calcium channel blocker), as well as the inhibition of calcium-induced tracheal contraction by curine, strongly suggests that this alkaloid modulates the allergic response through interference with calcium-dependent mechanisms (Ribeiro-Filho et al. 2013). The anti-allergic effect of curine was also demonstrated in a murine model of mast cell activation. The *in vivo* treatment with the alkaloid inhibited the scratching behavior and the anaphylactic shock reaction induced by compound 48/80, a substance that induces mast cell degranulation. Furthermore, the *in vitro* treatment of antigen-challenged RBL cells with curine or verapamil inhibited the production of lipid mediators that are crucially associated with allergic processes (Ribeiro-Filho et al. 2014). It is worthwhile mentioning that the curine oral treatment of mice, for seven consecutive days, did not induce evident toxicity related to physical, behavioral, histological, hematological, and biochemical parameters (Ribeiro-Filho et al. 2013; Leite et al. 2014). Recently, we showed that curine prevented macrophage activation as well as recruitment and activated neutrophils in the LPS-induced pleurisy model (Ribeiro-Filho et al. 2019).

These accumulated pieces of evidence put out curine (**1**) as a potent anti-inflammatory and anti-allergic alkaloid with low toxicity. However, the mechanisms underlying its effects are poorly understood. Therefore, this study aimed to investigate alkaloid curine in the LPS-induced acute lung inflammation model to elucidate its mechanism of action.

Experimental

Curine Preparation

The stem bark of *Chondrodendron platyphyllum* (A.St.-Hil.) Miers, Menispermaceae, according to registration number AAF4E49 in the Sistema Nacional de Gestão do Patrimônio Genético e do Conhecimento Tradicional Associado (SISGEN) was sprayed in a HARLEY-type mill and subjected to a series of extractions under exhaustive percolation with 95° GL ethanol for 3 to 4 days. The extract was vacuum concentrated at 50 to 60 °C, giving the crude ethanolic extract. The ethanolic extract was acidified (3% HCl solution) and filtered through celite. This acid solution was alkalized with cold ammonium hydroxide to (NH_4OH) to pH 8 and exhaustively extracted with chloroform until a negative result was obtained with the Mayer and Dragendorff reagents. The chloroform phase was dried with anhydrous sodium sulfate and concentrated on rotavapor (50 °C) to obtain the total tertiary alkaloid (TTA) fraction, which was subjected to column chromatography and analytical thin-layer chromatography for the isolation of curine (**1**), as previously described (Dias et al. 2002).

Animals

Male BALB/c isogenic mice (6 to 8 weeks) weighing between 20 and 25 g were supplied by Prof. Dr. Thomas George from the animal facilities of Instituto de Pesquisa em Fármacos e Medicamentos, UFPB, João Pessoa, PB, Brazil. Six animals represented each experimental group. The animals were euthanized by intramuscular (*i.m.*) administration of an anesthetic solution containing 29 mg/ml of ketamine and 1.91 mg/ml of xylazine in saline (NaCl 0.9%).

Acute Lung Injury Model

The experimental model of acute lung injury was developed and adapted from previously described methodologies (do Nascimento Xavier et al. 2019). On day zero (0), the mice were challenged by nasal instillation (*i.n.*), with a lipopolysaccharide solution (LPS—2.5 mg/kg, *E. coli* 0111: B4, Sigma-Aldrich, USA) in saline. At intervals of 1, 24, and 48 h after the challenge, the animals were orally treated by gavage (*p.o.*) with curine (**1**) at doses of 1.25, 2.5, 5, and 10 mg/kg. After 72 h of the challenge, the animals were euthanized, and the biological material was collected for the analysis of immunological parameters. The basal group did not receive the LPS challenge but was treated with saline solution (*i.n.*).

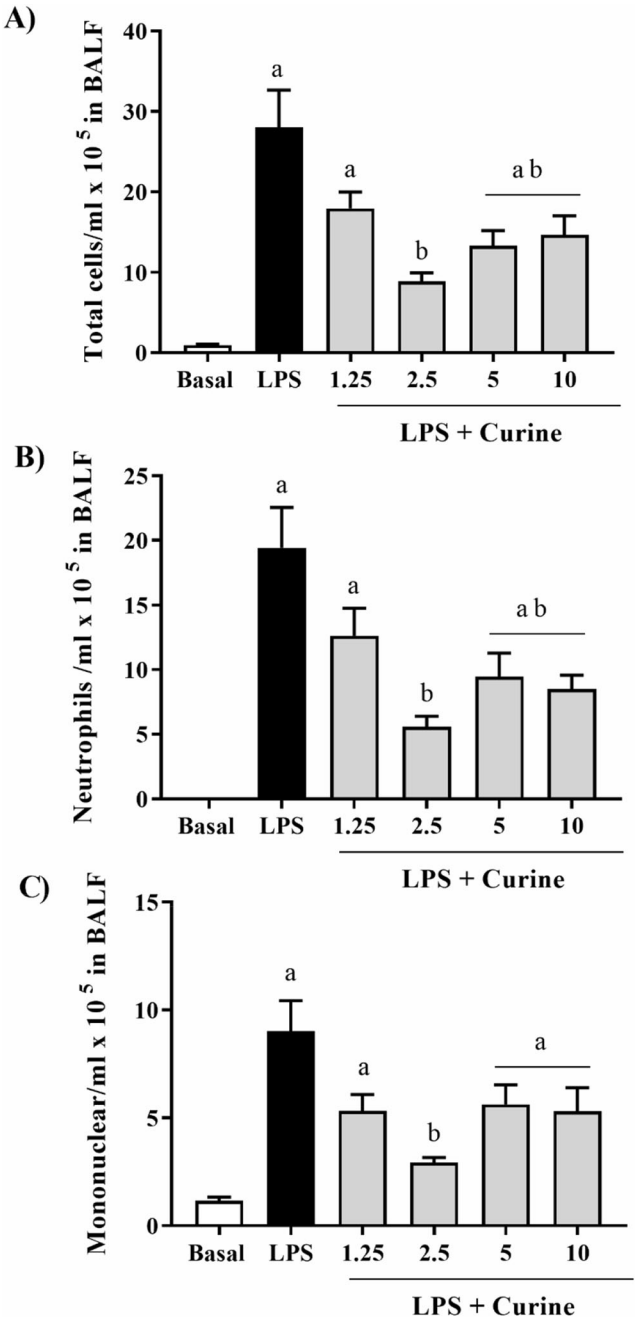

Fig. 1 Curine (**1**) effect on inflammatory cell migration to the lung cavity in lipopolysaccharide-induced acute lung injury (LPS-ALI). Male BALB/c mice ($n = 6$) were challenged with lipopolysaccharide (LPS) and treated orally (*p.o.*) with curine (1.25, 2.5, 5.0, and 10 mg/kg) 1, 24, and 48 h after the LPS challenge. After 72 h, the bronchoalveolar lavage fluid (BALF) was collected, and the total inflammatory cells (**A**) were counted with Turk's solution. The cell suspension was cytocentrifuged, and neutrophils (**B**) and mononuclear cells (**C**) were counted with the Panotic stain. Results were expressed as mean ± standard error of the mean and statistically analyzed by one-way ANOVA followed by the Tukey test, where values of (a)$p < 0.05$ were considered significant when compared to the basal group and (b)$p < 0.05$, when compared to the LPS group. Experiments were performed in triplicate

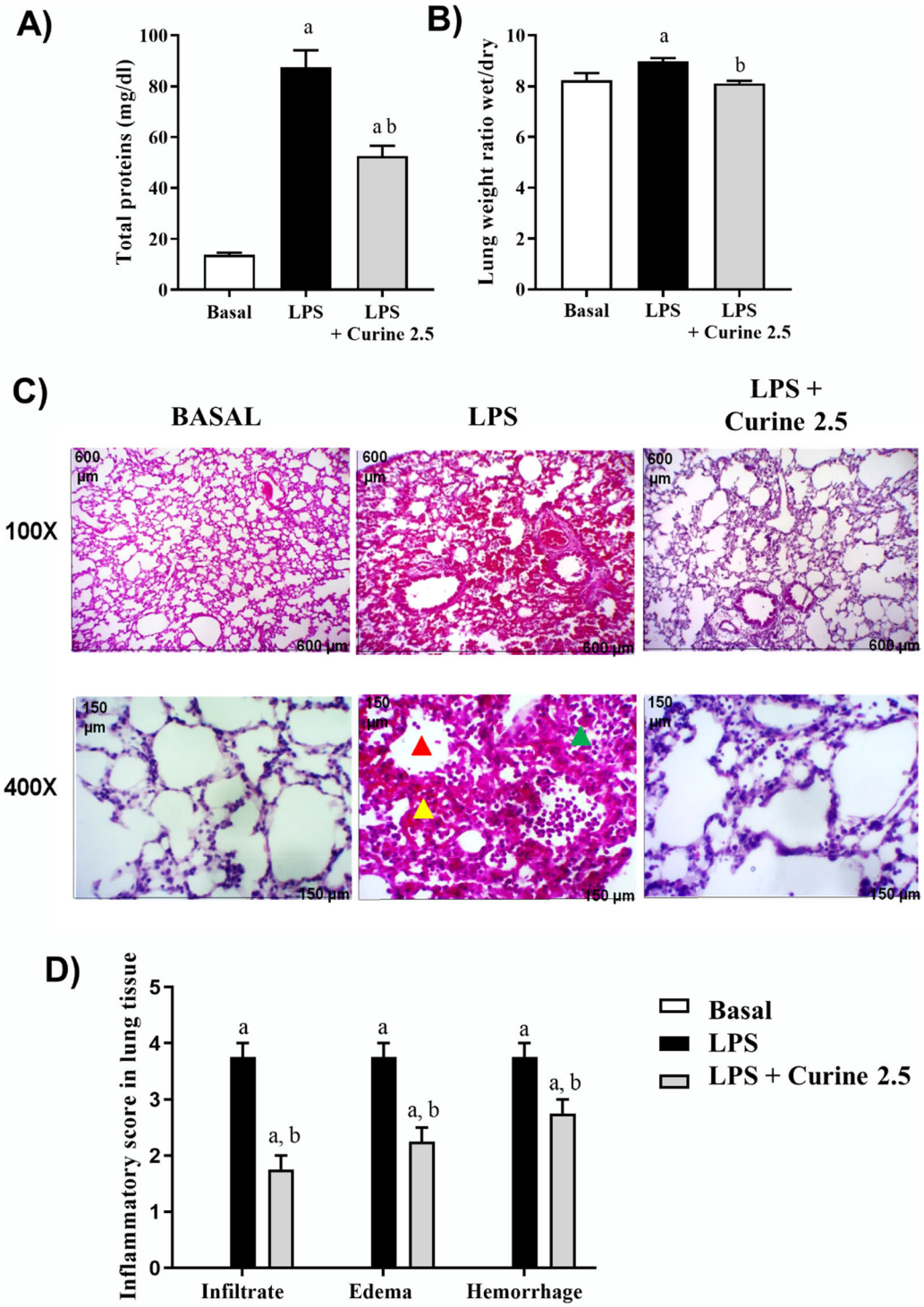

Fig. 2 Effect of curine (**1**) on vascular permeability, protein total leakage, lung edema, and lung histopathological aspects in the lipopolysaccharide-induced acute lung injury (LPS-ALI). Male BALB/c mice (n = 6) were challenged with lipopolysaccharide (LPS) and treated orally ($p.o.$) with curine (2.5 mg/kg) 1, 24, and 48 h after the LPS challenge. **A** After 72 h, the bronchoalveolar lavage fluid (BALF) was collected and the protein contents were measured by the Sensiprot test at 600 nm. **B** Lungs were collected to determine the wet/dry weight ratio. **C** Photomicrographs of tissue sections and inflammatory parameters as cell infiltrate (green triangle); edema (red triangle) and hemorrhage (yellow triangle) were observed at optical microscopy (100×, 600 µm) and 400× (150 µm). **D** Inflammatory scores: 0, absence of histological changes; 1, mild histological changes (less than 25% of the analyzed field); 2, moderate histological changes (from 25 to 49% of the analyzed field); 3, marked histological changes (from 50 to 75% of the analyzed field), and 4, very marked changes (more than 75% of the analyzed field). Results were expressed as mean ± standard error of the mean and statistically analyzed by one-way ANOVA followed by the Tukey test, where values of (a)$p < 0.05$ were considered significant when compared to the basal group and (b)$p < 0.05$ when compared to the LPS group. Experiments were performed in triplicate

Cell Quantification

The inflammatory cell migration to the lung was measured in the bronchoalveolar lavage fluid (BALF). For the collection of the BALF, 1.5 ml of ice-cold $HBSS^{+/-}$ was injected into the animal's lung through the trachea and the collected fluid was transferred to test tubes and stored at 4 °C. The cell counting was performed in a hemocytometric chamber at an optical microscope (40×; BX40, Olympus). The supernatants were used for the measurement of cytokines and total proteins. Differential cell counts were performed using cytospin (Fanen, São Paulo, SP, Brazil, Mod 2400) slides fixed and stained using the panoptic method (Panotic Kit, Renylab). Each slide was traversed until the counting of 100 cells, using the immersion objective (100×) of an optical microscope (do Nascimento Xavier et al. 2019).

Total Protein Quantification

The concentration of total proteins in the BALF of the different animal groups was quantified by the colorimetric method of the red pyrogallol dye using the Sensiprot kit (Labtest, Minas Gerais, MG, Brazil) according to the manufacturer's instructions. Pyrogallol red reacts with sodium molybdate to form a complex that, when combined with protein in an acid medium, develops a blue-colored chromophore with a maximum absorption of 600 nm. The resulting absorbance is directly proportional to the concentration of proteins in the sample (do Nascimento Xavier et al. 2019).

Wet and Dry Lung Weight Ratio

The lung of each animal was removed and immediately weighed to determine the "wet" weight. Then, the lung was placed in the oven at 60 °C for 48 h and weighed to assess the "dry" weight. The pulmonary edema index was calculated through the wet/dry weight ratio of the lung tissues, as previously described (Jiang et al. 2015).

Lung Histological Analysis

To assess the lung histological aspect, the organ was collected 72 h after the LPS challenge (endpoint) and fixed in buffered formalin. Then, the lung was hydrated and dehydrated with ethyl alcohol, xylol, and liquid histological paraffin (Erviegas, São Paulo, SP) to obtain the paraffin "block" containing the tissue fragment. Histological sections of 5 μm thick were obtained with the aid of a microtome (SP Labor 300). The tissue sections that adhered to the slides were stained with hematoxylin and eosin, to assess the pulmonary architecture and the general parameters of the inflammatory process. The morphological analysis was performed through scores correlating with the clinical aspects, and the final score values were determined according to the extent of the lesions. The inflammatory parameters were scored from 0 to 4 according to the extent of the tissue alterations as cell infiltration, edema formation and the presence of hemorrhagic foci, and the thickening of the alveolar septum, as well as the diffuse alveolar damage. The score values were determined considering the degree of histological changes in these parameters as follows: 0, absence of histological changes; 1, mild changes corresponding to less than 25%; 2, moderate changes ranging between 25 and 49%; 3, marked changes corresponding to an alteration of 50 to 75%; and 4, very marked changes, in which the parameter was altered in more than 75%. The tissue changes were evaluated in all fields of each slide in a double-blind manner, and four slides were analyzed (do Nascimento Xavier et al. 2019).

Cytokine Quantification

The cytokine production (TNF-α, IL-1β, and IL-6) was analyzed by ELISA according to the manufacturer's instructions) in the BALF supernatants (eBioscience, San Diego, CA).

Toll-Like Receptor 4 and Nuclear Factor κB (p65) Analyses

Flow cytometry analyses of the BALF allow the distinction of heterogeneous cell populations based on parameters such as "forward-scattered light" (FSC) and "side-scattered light" (SSC), which distinguish cells by size (light diffraction-FSC) and granularity (light diffusion-SSC), respectively. The granulocyte population of all animals was quantified in the BALF (van Rijt et al. 2004), and the toll-like receptor 4 (TLR4) receptor and the p65 portion of the transcription factor NFκB expressions were analyzed. About 5×10^5cells/ml on ice $HBSS^{+/-}$ were submitted to the flow cytometry (FACSCanto ™ II, BD, USA; FACS Diva 6.1. software) and determined the FSC and SSC parameters and for each marker specific antibodies, anti-TLR-4 and anti-nuclear factor κB (NF-κB) (p65), and fluorescent labeling in 10.000 events. The specific protocol for each marking was performed according to the kit manufacturer's recommendations (Bioscience, Inc. Science Center Drive, San Diego, CA, USA). For TLR-4(PE) labeling, a filter of 564–606 nm was used, and for the NFκB (p65) (PerCP-Cy5.5), a filter of 670–735 nm was used.

Molecular Docking

The TLR4/myeloid differentiation factor 2 (MD-2) selected for molecular coupling was acquired from the protein database PDB (https://www.rcsb.org/pdb/home/home.do) (Abraham et al. 2015), under PDB code ID 3FXI. For docking analysis, curine (**1**) was inserted in the SDF format and all water

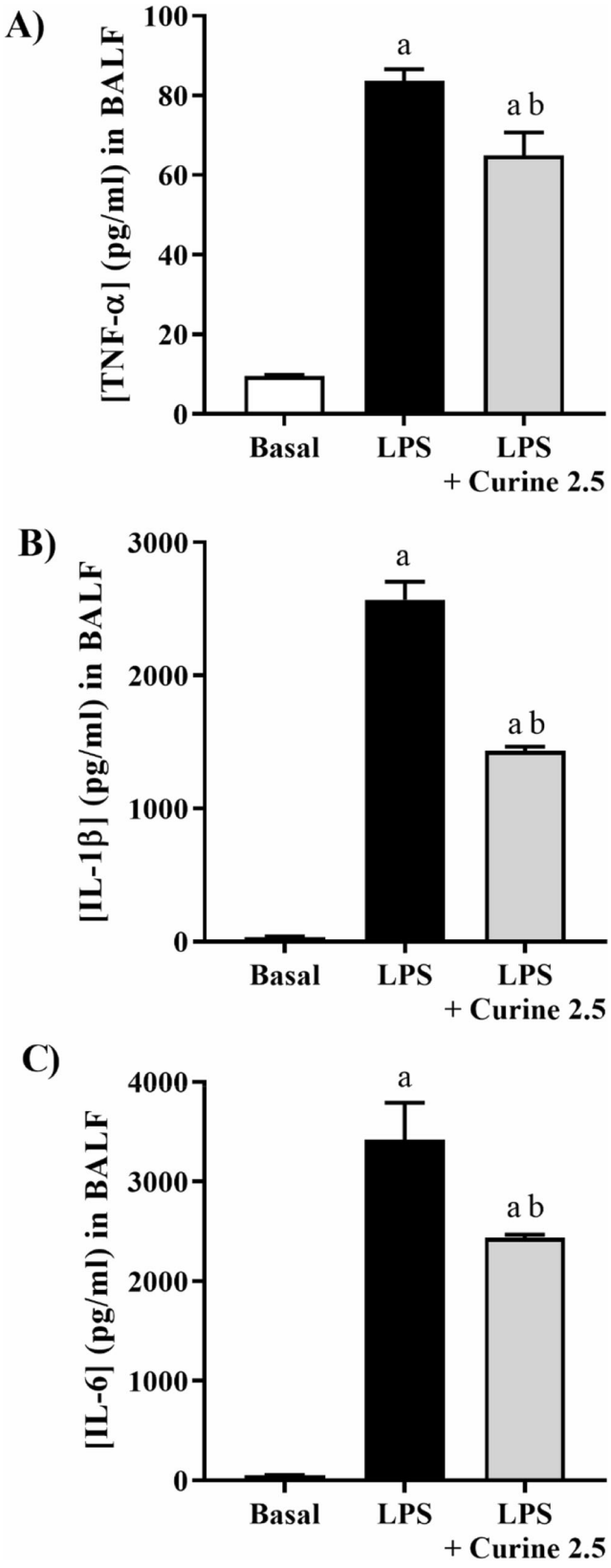

Fig. 3 Effect of curine (**1**) in the cytokine production in the lipopolysaccharide-induced acute lung injury (LPS-ALI). Male BALB/c mice ($n = 6$) were challenged with lipopolysaccharide (LPS) and treated orally (*p.o.*) with curine (2.5 mg/kg) 1, 24, and 48 h after the LPS challenge. After 72 h, the bronchoalveolar lavage fluid (BALF) was collected and the cytokine levels were measured by ELISA. **A** [TNF-α], **B** [IL-1β], and **C** [IL-6]. Results were expressed as mean ± standard error of the mean and statistically analyzed by one-way ANOVA followed by the Tukey test, where values of (a)$p < 0.05$ were considered significant when compared to the basal group and (b)$p < 0.05$ when compared to the LPS group. Experiments were performed in triplicate

molecules and cofactors removed when they were not close to the active site. The Molegro Virtual Docker v.6.0.1 (MVD) program (Bitencourt-Ferreira and de Azevedo 2019) was used to calculate the binding energy. For the coupling procedure (receiver-ligand), a GRID radius of 15 Å and resolution of 0.30 were used covering the binding site, defined using a known ligand for each enzyme. The model was designed to perform the adjustment with the characteristics expected between the ligand and the enzyme, using the heuristic search algorithm that combines the differential evolution and the crystallographic ligand as a model. The cavity prediction algorithm (Moldock) and the Moldock score function were selected to obtain the results (Thomsen and Christensen 2006).

Simulations of Molecular Dynamics

Molecular dynamics simulations were performed to estimate the flexibility of interactions between proteins and ligands using the GROMACS 5.0 software (Berendsen et al. 1995). The topology was prepared using the GROMOS96 54a7 force field in GROMACS. The molecular dynamics simulation was performed using the SPC water model with an extended point load in a cubic box (Pettersen et al. 2004). The system was neutralized by the addition of ions (Cl^- and Na^+) and minimized to remove bad contacts between complex molecules and the solvent. The system was also balanced at 300 K using the V- rescale algorithm at 100 ps represented by NVT (constant number of particles, volume, and temperature), followed by equilibrium at 1 atm of pressure using the Parrinello-Rahman algorithm as NPT (constant pressure numeric particles and temperature) up to 100 ps. DM simulations were performed in 5,000,000 steps at 10 ns. To determine the flexibility of the structure and whether the complex is stable close to the experimental structure, the mean square root displacement (RMSD) of all Cα atoms was calculated in relation to the starting structures. Residual fluctuations (RMSF) were also analyzed to understand the role of residues near the receptor binding site. The RMSD and RMSF graphs were generated in the Grace software (http://plasma-gate.weizmann.ac.il/Grace/), and the protein and ligands were visualized in the UCSF Chimera (Orlando and Malkowski 2016).

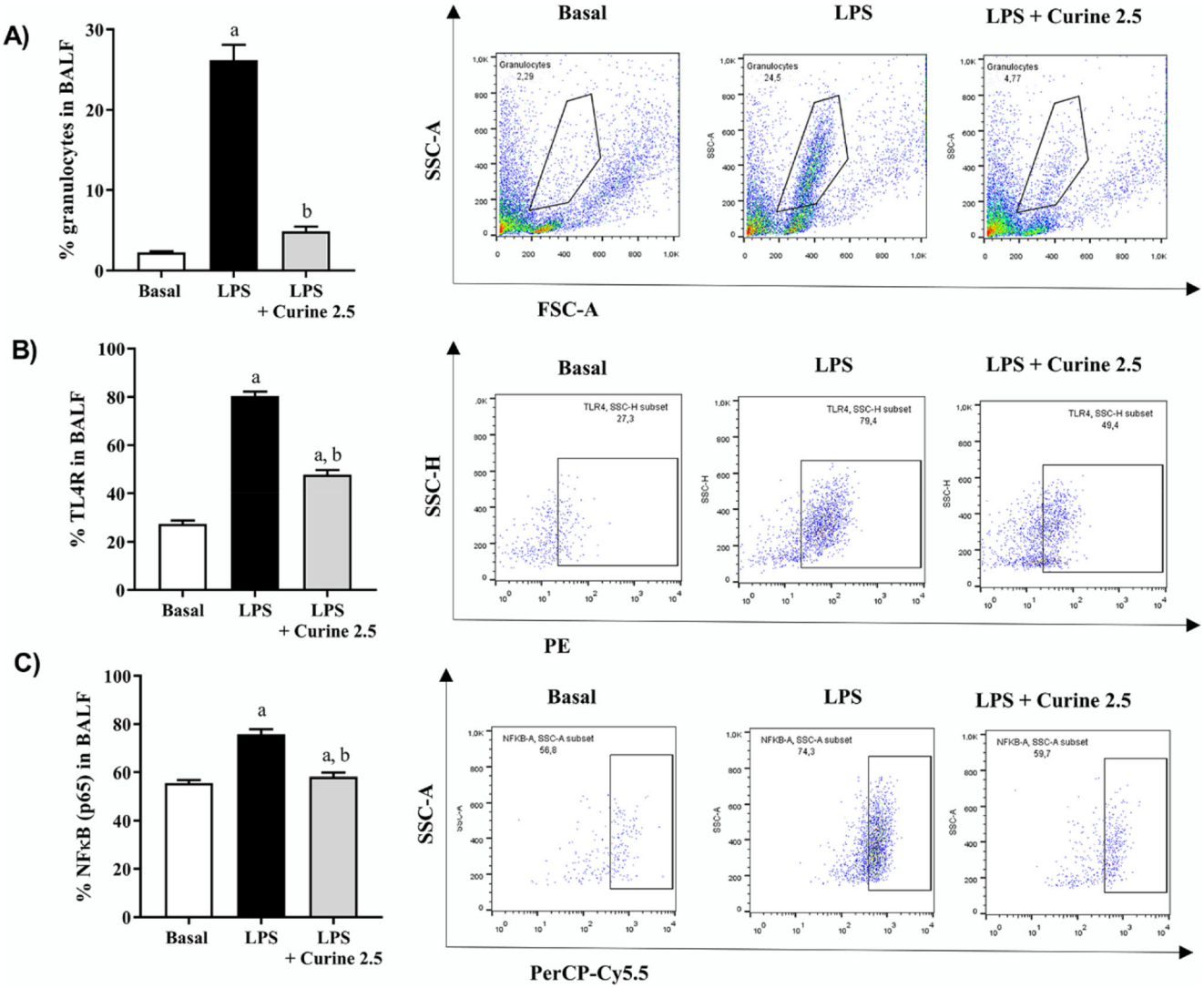

Fig. 4 Effect of curine (**1**) on the Toll-Like 4 receptor (TLR4) expression and NF-κB(p65) activation. Male BALB/c mice ($n = 6$) were challenged with lipopolysaccharide (LPS) and treated orally (*p.o.*) with curine (2.5 mg/kg) 1, 24, and 48 h after the LPS challenge. After 72 h, the bronchoalveolar lavage fluid (BALF) was collected and the cell suspension was analyzed by flow cytometric analysis (FSC Forward Scatter, by light diffraction) and cytoplasmic granularity or complexity (SSC Side Scatter, by light diffusion). **A** Percentage of granulocytes, **B** TL4R (PE) expression, **C** p65 portion phosphorylation of the NFκB Transcription Factor (PerCP-Cy5-5). Results were expressed as mean ± standard error of the mean and statistically analyzed by one-way ANOVA followed by the Tukey test, where values of (a)$p < 0.05$ were considered significant when compared to the basal group and (b)$p < 0.05$ when compared to the LPS group. Experiments were performed in triplicate

Statistical Analyses

The data were analyzed by GraphPad Prism© version 5.0 software (GraphPad Software, San Diego, CA, USA). Results were expressed as mean ± standard error of the mean (e.p.m.) and statistically analyzed by one-way ANOVA followed by the Tukey test, where values of $p < 0.05$ were considered significant.

Results and Discussion

Curine (**1**), a bisbenzylisoquinoline alkaloid, was identified as a promising anti-inflammatory molecule with the potential to become a medicine for the pulmonary inflammatory process treatment. However, the molecular mechanisms underlying its effects remain to be clarified. Thereby, the goal of this study was to demonstrate its mechanisms of action in a well-established, *in vivo* lung inflammatory process induced by lipopolysaccharide (LPS) in mice (Medeiros et al. 2011; Leite et al. 2014; Dantas et al. 2015; Ribeiro-Filho et al. 2013, 2019).

Effect on Inflammatory Cell Recruitment

The inflammatory cell profile in the bronchoalveolar lavage fluid (BALF) of the animal groups is shown in Fig. 1. The animals from the LPS group showed an increase ($p < 0.05$) in

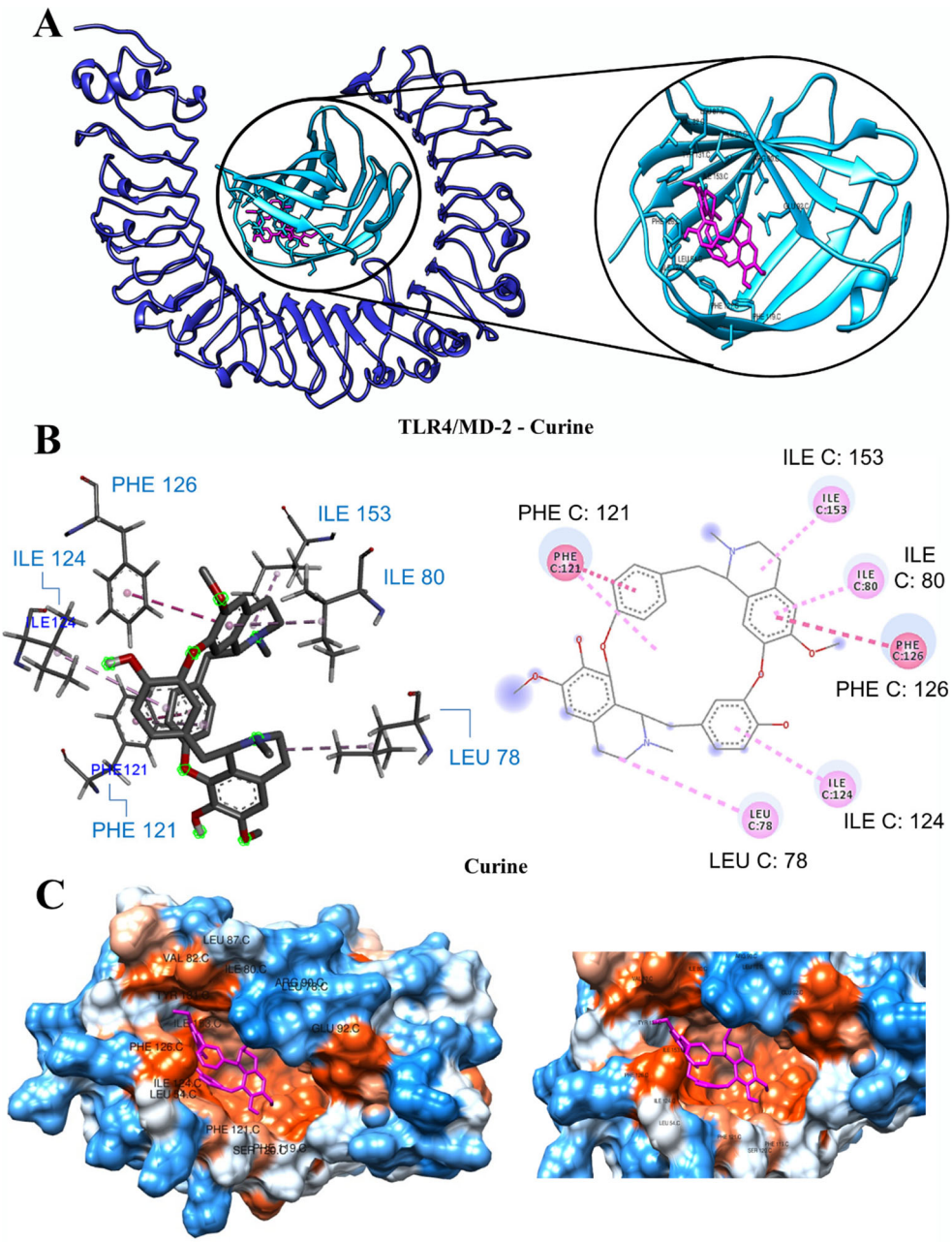

Fig. 5 Effect of curine (**1**) on the TLR4/MD-2 protein complex. **A** General structure of the TLR4/MD-2-curine complex (dark blue for TLR4, light blue for MD-2 and curine). **B** 3D and 2D interactions of the MD-2 complex and curine. The interaction of MD-2 residues with hydrophobic chains of curine is labeled in blue. **C** Representation of MD-2 surface. Positively and negatively charged residues are in blue and orange, respectively

the number of inflammatory cells, mainly neutrophils, in the lung cavity (Fig. 2). Indeed, in these animals, the number of neutrophils increased about twenty times as compared to the animals from the basal group (19.42 ± 3.12 vs 0.01 ± 0.01, respectively) (Fig. 2B). However, animals LPS-challenged and treated with curine (2.5, 5, or 10 mg/kg) presented a decreased ($p < 0.05$) number of neutrophils, corresponding to 72, 52, and 57%, respectively (Fig. 2B). Indeed, the number of neutrophils of the curine (2.5 mg/kg)-treated animals was similar to that of the animals from the basal group indicating the reestablishment of lung homeostasis. Therefore, the dose of 2.5 mg/kg was chosen to proceed with the investigation of the curine effect in the ALI model.

Effect on Pulmonary Edema

The effect of curine on pulmonary edema was assessed by quantifying the BALF protein content (mg/dl) and by the lung weight ratio. The LPS group showed a sixfold increase ($p < 0.05$) in the total protein content as compared to the basal group (87, 44 ± 6.65 vs 13.86 ± 0.769, respectively) (Fig. 2A). The curine treatment promoted a decrease ($p < 0.05$) of the protein exudate in about 40% in comparison with the LPS group (Fig. 2A), indicating the diminishing of pulmonary edema formation. This finding corroborated with the wet/dry (W/D) lung weight ratio, which shows that curine reduced it by about 10% (Fig. 2B).

Effect on Pulmonary Tissue

The histological aspect of the lung tissues of the animals is shown in Fig. 2C, D. The lung tissue of animals of the LPS group showed an intense cellular infiltration in the alveoli (green triangle), edema with the presence of hyaline membrane and thickening of the alveolar wall (red triangle), hemorrhage (red blood cells), vasodilation, and an increase of blood flow in the alveolar capillaries (yellow triangle). The inflammatory score of the tissue morphological changes was observed with cellular infiltration demonstrating an intense inflammatory process on these animals as compared to the basal group. The curine treatment of LP-challenged animals promoted a reduction ($p < 0.05$) of 54% of inflammatory cell infiltration, 40% of edema, and 27% of hemorrhage.

Effect on Cytokine Production

The BALF concentration (pg/ml) of TNF-α, IL-1β, and IL-6 is shown in Fig. 3A–C. Animals of the LPS group presented ($p < 0.05$) increased amounts of TNF-α (83.72 ± 2.81 *vs* 9.45 ± 0.35), IL-1β (2572 ± 135.4 *vs* 33, 37 ± 5.63), and IL-6 (342 ± 370.10 *vs* 48.37 ± 5.32) as compared to those of the basal group. The curine treatment of LPS-challenged animals inhibited ($p < 0.05$) the production of these cytokines in 23, 56, and 29%, respectively, indicating an anti-inflammatory effect of the alkaloid in LPS-induced ALI by modulating inflammatory cytokines.

The main piece of evidence of the current study was that curine protected the animal lung tissue from damage caused by LPS by reducing neutrophil migration, protein exudate, and edema formation. Besides, curine decreased the production of TNF-α, IL-1β, and IL-6, and downregulated the TLR-4/NF-κB signaling pathway. In this scenario, this study demonstrated the mechanism(s) of action of curine by using as a tool the experimental model of LPS-induced acute lung injury (ALI). ALI and its most severe form, acute respiratory distress syndrome (ARDS), are global health problems, with high morbidity and mortality rates. These diseases are characterized by an extensive lung inflammatory reaction mainly mediated by neutrophils and rupture of the alveolar-capillary barrier leading to severe impairment of gas exchange. Indeed, activated neutrophils release multiple toxic mediators as reactive oxygen species (ROS), proteases, and pro-inflammatory cytokines damage the lung tissue (Bhattacharya and Matthay 2013). The LPS-challenged animals treated with curine presented a decrease of neutrophils in the lung and, by histological analyses and the semi-quantitative scoring system, demonstrated that curine decreased hemorrhage, edema, and the thickening of the alveolar septum, as well as the narrowing of the alveolar spaces leading to improvement of the lung tissue damage.

Effect on TLR4 and NFκB (p65) Expression

The curine treatment decreased the percentage of granulocytes (26.20% ± 1.92 *vs* 4.90% ± 0.58) compared to the LPS group (Fig. 4A). Indeed, these animals presented a decrease ($p < 0.05$) of the TRL4 frequency in this cell population (80.5% ± 1.81 *vs* 47.8% ± 1.91) (Fig. 4B). Since the TRL4/MD2 signaling axis is associated with NF-κB(p65) activation during the production of inflammatory cytokines, the phosphorylated p65 portion of the NFκB was looked at in curine-treated animals. Figure 4C shows that the alkaloid reduced the frequency of expression of this transcriptional factor (75.80% ± 2.15 *vs* 58.20% ± 1.62, $p < 0.05$) as compared to the LPS group.

LPS binds to the TLR-4/MD2 complex and triggers the intracellular signaling cascades culminating with the NFκB pathway activation, and transcription of a wide variety of genes, including those of inflammatory cytokines (Thomsen and Christensen 2006). In this study, we demonstrated that curine decreased the expression of TLR-4 and diminished the NFκB (p65) phosphorylation on granulocytes from the BALF, allowing us to suggest that at least one way that curine protects the animals from lung damage caused by LPS in ALI is by decreasing the expression of TLR-4 and downregulating the NFκB(p65) pathway.

Effect on TLR2/MD2 Complex

The TLR4/MD-2 protein complex recognizes and binds LPS to induce an innate immune response. Molecular docking demonstrated that curine coupled with a binding energy of -99.19 kcal/mol to the MD2 protein cavity mediated by several hydrophobic interactions. Figure 5A–C shows the curine hydrophobic interactions with amino acids Leu78, Ile80, Phe121, Ile124, Phe126, and Ile152. Also, the molecular dynamic simulation investigated whether curine might be binding to MD-2 under the influence of water solvent, ions, temperature, and pressure. Flexibility and changes in the MD-2 structure were also investigated. The RMSD analysis of MD2 showed that the protein reached fluctuation ranging from 0.3 to 0.45 nm in size in 10 ns, with stability after 6 ns, and the MD2/curine complex was stable over the 10 ns allowing the alkaloid to remain strongly bound to the active site of the receptor. Besides, the RMSD of curine was steady throughout the dynamic's simulation. Thereby, the residue flexibility of each amino acid of the MD-2 was calculated by the mean square root fluctuations (RMSF). Amino acid residues above 0.3 nm/RMSF are considered with fluctuations and give the flexibility of the protein structure. Therefore, among the 150 amino acids present in the protein, only amino acids 111 and

158 contributed to the conformational change of the MD2/curine complex. However, in the non-complexed MD2, high fluctuations were observed in amino acids 41, 58, 69, 84, 85, 122, 128, 157, and 158. Two of these amino acids (K122 and K128) are present in the active site and are essential for the recognition of LPS. Therefore, none of the amino acids responsible for the structural change of the complexed protein is part of the active site, and the active site is stable. When analyzed through graphic programs, the MD2/curine complex presented small conformational changes as identified by the RMSD values, and some connections in the docking were lost. However, other strong bonds were formed with amino acids Lys104, 105Gly, and Tyr113.

Conclusions

Therefore, in this study, we demonstrated that curine (**1**) reduced the inflammatory process in ALI dependent of neutrophil and decreased the production of the pro-inflammatory cytokines and edema with the improvement of the alveolar-capillary barrier by downregulating the TLR/MD-2/NF-kB signaling pathway. Also, this alkaloid blocks the LPS binding to the MD-2 chain, a protein that complexes with the TLR-4 receptor. *In silico* analysis demonstrated that curine was able to form several hydrophobic interactions with amino acids Leu78, Ile80, Phe121, Ile124, Phe126, and Ile152 present in the MD-2 chain, and the curine/MD-2 complex is stable, which favors the permanence linkage between those molecules. These data point out that curine is a promising candidate for drug development and further testing in clinical trials to treat acute respiratory distress syndrome.

Authors Contribution MRP, LAMPF, and LKDPF outlined and designed the experiments, wrote the original draft, and revised and edited the manuscript for submission. LAMPF and LKDPF performed the experimental model of ALI. LAMPF, LKDPF, and LML performed the ELISA protocol. LAMPF, LKDPF, and TMM performed the flow cytometry protocol. FAAFG performed the lung histology. MRP, LAMPF, and LKDPF analyzed the data. MSM and MTS performed the molecular docking and molecular dynamics simulations. JRF reviewed the manuscript. CSD was responsible for the alkaloid curine extraction and purification and made it available for the study. MRP was responsible for conceptualization, visualization, resources, funding acquisition, project administration, supervision, and writing—review and editing. All the authors have read the final manuscript and approved the submission.

Funding This study was sponsored by the Coordenação de Aperfeiçoamento de Pessoal de Nível Superior - Brasil (CAPES)-Finance Code 001 and CNPq (Conselho Nacional de Desenvolvimento Científico e Tecnológico - Brasil).

Declarations

Protection of Human and Animal Subjects The authors declare that no experiments were performed on humans. All studies were conducted by following the guidelines of the National Animal Experimentation Control Council (CONCEA) and adhered strictly to the guidelines of the Brazilian Law (n°. 11.794/2008) which establishes rules for use and care of laboratory animals. The Committee on Ethics in Uses of Animals (CEUA/UFPB) approved the experimental procedures under certificate n° 7316150420. The used animals were purchased from the Animal Production Unit of the Institute for Research on Drugs and Medicines (IPeFarM) of the Federal University of Paraíba, João Pessoa, PB, Brazil.

Conflict of Interest The authors declare no competing interests.

References

Abraham MJ, Murtola T, Schulz R, Páll S, Smith JC, Hess B, Lindah E (2015) Gromacs: high performance molecular simulations through multi-level parallelism from laptops to supercomputers. SoftwareX 1–2:19–25. https://doi.org/10.1016/j.softx.2015.06.001

Albiger B, Dahlberg S, Henriques-Normark B, Normark S (2007) Role of the innate immune system in host defence against bacterial infections: focus on the Toll-like receptors. J Intern Med 261:511–528. https://doi.org/10.1111/j.1365-2796.2007.01821.x

Bellani G, Laffey JG, Pham T, Fan E, Brochard L, Esteban A, Gattinoni L, Van Haren FMP, Larsson A, McAuley DF, Ranieri M, Rubenfeld G, Thompson BT, Wrigge H, Slutsky AS, Pesenti A (2016) Epidemiology, patterns of care, and mortality for patients with acute respiratory distress syndrome in intensive care units in 50 countries. J Am Med Assoc 315:788–800. https://doi.org/10.1001/jama.2016.0291

Berendsen HJC, van der Spoel D, van Drunen R (1995) GROMACS: a message-passing parallel molecular dynamics implementation. Comput Phys Commun 91:43–56. https://doi.org/10.1016/0010-4655(95)00042-E

Bhattacharya J, Matthay MA (2013) Regulation and repair of the alveolar-capillary barrier in acute lung injury. Annu Rev Physiol 75:593–615. https://doi.org/10.1146/annurev-physiol-030212-183756

Bitencourt-Ferreira G, de Azevedo WF (2019) Molegro virtual docker for docking. In: Methods in molecular biology. Humana Press Inc., pp. 149–167. https://doi.org/10.1007/978-1-4939-9752-7_10

Cheung OY, Graziano P, Smith ML (2017) Acute lung injury, 3rd ed. Practical pulmonary pathology: a diagnostic approach A Volume in the Pattern Recognition Series. Elsevier Inc. https://doi.org/10.1016/B978-0-323-44284-8.00006-5

Dantas BB, Faheina-Martins GV, Coulidiati TH, Bomfim CCB, Da Silva DC, Barbosa-Filho JM, Araújo DAM (2015) Effects of curine in HL-60 leukemic cells: cell cycle arrest and apoptosis induction. J Nat Med 69:218–223. https://doi.org/10.1007/s11418-014-0881-5

Dias CS, Barbosa-Filho JM, Lemos VS, Côrtes SF (2002) Mechanisms involved in the vasodilator effect of curine in rat resistance arteries. Planta Med 68:1049–1051. https://doi.org/10.1055/s-2002-35662

do Nascimento Xavier BM, Ferreira LAMP, Ferreira LKDP, Gadelha FAAF, Monteiro TM, de Araújo Silva LA, Rodrigues LC, Piuvezam MR (2019) MHTP, a synthetic tetratetrahydroisoquinoline alkaloid, attenuates lipopolysaccharide-induced acute lung injury via p38MAPK/p65NF-κB signaling pathway-TLR4 dependent. Inflamm Res 68:1061–1070. https://doi.org/10.1007/s00011-019-01291-3

Fan E, Brodie D, Slutsky AS (2018) Acute respiratory distress syndrome advances in diagnosis and treatment. JAMA 319:698–710. https://doi.org/10.1001/jama.2017.21907

Guedes DN, Barbosa-Filho JM, Lemos VS, Côrtes SF (2002) Mechanism of the vasodilator effect of 12-*O*-methylcurine in rat aortic rings. J Pharm Pharmacol 54:853–858. https://doi.org/10.1211/0022357021779032

Jiang Q, Yi M, Guo Q, Wang C, Wang H, Meng S, Liu C, Fu Y, Ji H, Chen T (2015) Protective effects of polydatin on lipopolysaccharide-induced acute lung injury through TLR4-MyD88-NF-κB pathway. Int Immunopharmacol 29:370–376. https://doi.org/10.1016/j.intimp.2015.10.027

Leite FC, Ribeiro-Filho J, Costa HF, Salgado PRR, Calheiros AS, Carneiro AB, De Almeida RN, Dias CDS, Bozza PT, Piuvezam MR (2014) Curine, an alkaloid isolated from *Chondrodendron platyphyllum* inhibits prostaglandin E2 in experimental models of inflammation and pain. Planta Med 80:1072–1078. https://doi.org/10.1055/s-0034-1382997

Medeiros MAA, Pinho JF, De-Lira DP, Barbosa-Filho JM, Araújo DAM, Cortes SF, Lemos VS, Cruz JS (2011) Curine, a bisbenzylisoquinoline alkaloid, blocks L-type Ca 2+ channels and decreases intracellular Ca 2+ transients in A7r5 cells. Eur J Pharmacol 669:100–107. https://doi.org/10.1016/j.ejphar.2011.07.044

Orlando BJ, Malkowski MG (2016)Substrate-selective inhibition of cyclooxygeanse-2 by fenamic acid derivatives is dependent on peroxide tone. J Biol Chem 291:15069–15081. https://doi.org/10.1074/jbc.M116.725713

Petrovska BB (2012) Historical review of medicinal plants' usage. Pharmacogn Rev 6:1–5. https://doi.org/10.4103/0973-7847.95849

Pettersen EF, Goddard TD, Huang CC, Couch GS, Greenblatt DM, Meng EC, Ferrin TE (2004) UCSF Chimera - a visualization system for exploratory research and analysis. J Comput Chem 25:1605–1612. https://doi.org/10.1002/jcc.20084

Proudfoot AG, McAuley DF, Griffiths MJD, Hind M (2011) Human models of acute lung injury. Dis Model Mech 4:145–153. https://doi.org/10.1242/DMM.006213

Rezoagli E, Fumagalli R, Bellani G (2017) Definition and epidemiology of acute respiratory distress syndrome. Ann Transl Med 5:282. https://doi.org/10.21037/atm.2017.06.62

Ribeiro-Filho J, Calheiros AS, Vieira-de-Abreu A, de Carvalho KIM, da Silva MD, Melo CB, Martins MA, da Silva DC, Piuvezam MR, Bozza PT (2013) Curine inhibits eosinophil activation and airway hyper-responsiveness in a mouse model of allergic asthma. Toxicol Appl Pharmacol 273:19–26. https://doi.org/10.1016/j.taap.2013.08.015

Ribeiro-Filho J, Carvalho Leite F, Surrage Calheiros A, de Brito Carneiro A, Alves Azeredo J, Fernandes de Assis E, da Silva Dias C, Regina Piuvezam M, Bozza PT (2019) Curine inhibits macrophage activation and neutrophil recruitment in a mouse model of lipopolysaccharide-induced inflammation. Toxins 11:705. https://doi.org/10.3390/toxins11120705

Ribeiro-Filho J, Leite FC, Costa HF, Calheiros AS, Torres RC, De Azevedo CT, Martins MA, Da Silva DC, Bozza PT, Piuvezam MR (2014) Curine inhibits mast cell-dependent responses in mice. J Ethnopharmacol 155:1118–1124. https://doi.org/10.1016/j.jep.2014.06.041

Thomsen R, Christensen MH (2006) MolDock: a new technique for high-accuracy molecular docking. J Med Chem 49:3315–3321. https://doi.org/10.1021/jm051197e

van Rijt LS, Kuipers H, Vos N, Hijdra D, Hoogsteden HC, Lambrecht BN (2004) A rapid flow cytometric method for determining the cellular composition of bronchoalveolar lavage fluid cells in mouse models of asthma. J Immunol Methods 288:111–121. https://doi.org/10.1016/j.jim.2004.03.004

Yang CY, Chen CS, Yiang GT, Cheng YL, Yong SB, Wu MY, Li CJ (2018) New insights into the immune molecular regulation of the pathogenesis of acute respiratory distress syndrome. Int J Mol Sci 19:588. https://doi.org/10.3390/ijms19020588